Unsynchronized Ultrasound System for TDOA Localization

Alexander Ens and Leonhard M. Reindl
Department of Microsystems Engineering,
University of Freiburg, Germany
{alexander.ens, reindl}@imtek.uni-freiburg.de

Joan Bordoy, Johannes Wendeberg
and Christian Schindelhauer
Department of Computer Science,
University of Freiburg, Germany
{bordoy, wendeber, schindel}@informatik.uni-freiburg.de

***Abstract*—Indoor localization based on time difference of arrival (TDOA) has been recently a promising field of study. We consider the previously unsolved problem of locating a moving target receiver by using unsynchronized stationary beacons without requirement of manual calibration. Thus, the received signals and their time of arrival (TOA) have to be assigned to a beacon. Besides, in order to automatically calibrate the system it is required to estimate the time offsets between the senders, their positions and the initial receiver position.**

We present an approach to estimate all the variables of the scenario using the gradient descent and the Gauss-Newton method, two local optimization algorithms which use the derivative of a system of hyperbolic error equations. Besides, we present an ultrasound transmission system approach which fulfils the requirements of this scenario, being robust against multipath and estimating the reception time with high accuracy. In order to avoid interference by echoes the packet size is reduced by using two frequencies in Orthogonal Frequency Division Multiplex (OFDM). Further, the transmission system enables distinction of the beacons, as the ultrasound signals are used both for localization and for information transmission.

The simulations show the local optimization algorithms are capable of estimating the positions of the beacons, receivers and offsets. They require only a rough knowledge of the sender positions. Further, real experiments show that the timestamps are measured with a standard deviation of only 1.19 μs for a SNR of 10 dB, which corresponds to standard deviation of about 0.4 mm for the distance measurement.

***Index Terms*—OFDM, Ultrasound, Communication, Localization, Piezo, TDOA**

I. Introduction

In our everyday life it is important to know the actual position of things. The interests in localization services are growing and there are many possible applications (e.g. as navigation of shopping carts in super markets). Localization systems based on ultrasound are very cost effective, have a low complexity and simple hardware compared to radio frequency systems. Further, the position can be estimated with very high accuracy. While the speed of sound is about 10^6 times slower than the speed of light, the position can be determined by time delay of arrival (TDOA) methods with low sampling rates of the received signal and without an additional intermediate frequency mixer.

The disadvantage of ultrasound is the absorption and therefore the attenuation of the transmitted signal by the air. Further the attenuation increases with the frequency [1]. Hence, we use low frequency for the transmission within 40 kHz. Moreover, the sound noise from industry and traffic disturb the ultrasound. Another point that should be kept in mind, are the good reflections at walls and plane surfaces that cause additional echoes, which disturb the signal and reduces the signal-to-noise ratio (SNR) at the receiver.

Absolute localization is important for most applications. Especially management of goods in warehouses or customer localization in supermarkets [2]. While in outdoor scenarios GPS has been playing an important role, it lacks connectivity in indoor scenarios and its precision is in the order of meters. Laser localization systems are sensitive to dust and have a small coverage area [3]. Further, the system is very expensive, require a central processing unit and the amount of mobile tracked devices is limited. We present an absolute positioning system for indoor localization of goods or autonomous vehicles. Through the decentralized design, the localization is independent of the localized objects and of a central control unit. Further, each robot calculate the position. Hence, we can use unlimited devices for localization.

In this approach, multiple unsynchronized beacons are used to track the position of a moving receiver without requirement of manual calibration. Local optimization algorithms and statistical approaches are used to estimate the initial parameters of the scenario (sender positions, intervals...), which are afterwards used in recursive state estimation (unscented Kalman filter and particle filter). In order to estimate the initial values the receiver is required to stop in certain positions receiving at least one signal burst from every sender. Once the initial values are estimated the receiver can move continuously. To distinguish between more than one transmitter, the transmitted signals need additional information of the signal origin and therefore the identification of the transmitter. Then the receiver can determine the origin of the signal and map the time of arrival to the transmitter. A promising approach for this was demonstrated in [4]. The calculation of the position is then augmented from the TDOA problem to data transmission and TDOA.

Beacons can be distinguished by giving each transmitter a different frequency band for the data communication. However, broadband receivers are very expensive and the frequency bands are limited. Another modulation scheme is the chirp spread spectrum (CSS) [5]. The CSS modulation avoids destructive interference of the echoes at the receiver

978-1-4673-8054-6/14/$31.00 ©2014 IEEE

by linear frequency modulation and therefore the signal cannot disappear at the receiver. Another advantage of the CSS is the robustness against the Doppler shift and good detection of the center of the chirp sequence by correlation. Nevertheless, the modulated data is very low (1 kBaud) and we require high bandwidth components at the transmitter and receiver side. Hence, this increases the transmission duration and the costs of the system.

Another robust modulation scheme is the phase shift keying (PSK) [6], which includes the information in the phase. To reduce fast phase changes, the signal can be modulated by Gaussian Minimum Shift Keying (GMSK) [7]. Moreover, the frequency shift keying (FSK) can also be used for data modulation, though the bit error rate (BER) is higher than for PSK or π/4-QPSK [8].

II. Related Work

Table I shows the state-of-the-art indoor ultrasound localization systems, that use stationary mounted senders and receivers on mobile devices. All systems use synchronized beacons and therefore, the beacons have a second communication channel (backward channel) or they are connected by wire. The beacons are synchronized by a central unit or triggered by the mobile robots with a radio frequency (RF) channel (e.g. Bluetooth, Zigbee). Although our system has no backward channel and is unsynchronized.

To increase the data rate, modern system use orthogonal frequency division multiplex (OFDM) to spread the data stream onto multiple carrier [9]. The carriers are orthogonal and each can be modulated separately. We use OFDM with two carrier frequencies to achieve short pulse length.

Villadangos et al. [10] and Urena et al. [11] describe a localization system for indoor with stationary mounted senders at the ceiling and mobile receivers. Whereas the senders are connected by wire to a central control unit. This synchronizes the transmission of the beacons. Schweinzer et al. [12] describe a low cost ultrasound system also with central synchronized beacons at the ceiling. Ruiz et al. [13] and Medina et al. [14] use RF to synchronize the beacons and to measure the time-of-flight (TOF). Moreover, Kim et al. [15] combine the information from ToF with the angle-of-arrival (AOA) to achieve higher localization accuracy.

However, RF controlled system has the flaw of limited number of mobile devices, due to the second radio frequency control channel. Moreover, beacons with wired installation and central control units cause high installation costs. Indeed, new research enables localization without synchronized beacons. Saad et al. [16] shows a localization system with unsynchronized beacons at the ceiling and mobile receivers. However, they use AOA to compute the position and have to know the positions of the beacons. This results in relative high standard deviation of the estimated position, compared to TOF or T(D)OA based localization systems.

TDOA has been often used to track the position of a moving sender using stationary receivers. The algorithms used are squared or maximum likelihood estimators [17], particle filters [18], [19] or Kalman filters [20], [21]. We consider the inverted scenario where a moving receiver is located. This scenario has been solved in [22] using a weighted least squares procedure. Though, the receiver is assumed to have a simple trajectory. Besides, they take advantage of the receiver odometry measurements. In [23], [24] a least squares method is used to estimate the position of a moving ultrasound receiver with maximal velocities of 0.2 m/s. The intervals and the sender positions are assumed to be known beforehand. Furthermore, the receiver is assumed to receive signals from all the senders while remaining in the same position. This would lead to high positioning errors if the receiver moves at high velocity.

Wendeberg et al. [25] and Bordoy et al. [26] show the feasibility of reference and calibration free localization systems with TDOA. As a result, the mobile receivers have no information about the positions of the beacons and themself. Further, the beacons are unsynchronized and send in constant interval a pulse. Hence, the receiver has to estimate the positions of the beacons and their own position.

Table I
Comparison-of-ultrasound localization system with mobile receivers and stationary senders. (Not available data is denoted with NA)

Range	Methods	Beacons synchronized	Channel for synchronization	Ref
[m]	[Yes|No]	[Yes|No]	[No|RF|Central]	
4	TDOA	Yes	Central	[10]
4	TDOA	Yes	Central	[11]
4	TDOA	Yes	Central	[12]
NA	TDOA	Yes	Central	[24]
4	TOF, Odometry	Yes	RF	[13]
3	TOF, AOA Odometry	Yes	RF	[15]
5	TOF	Yes	RF	[14]
4	TOF, AOA	No	No	[16]
4	TDOA	No	No	this

III. System Components

A. Environment

The localization system consists of installed unsynchronized ultrasound senders on the ceiling and mobile devices with ultrasound receivers. The senders have only a simplex ultrasound communication and transmit in constant intervals short packages. Further, the packages include the identification number (ID) of the sender and the temperature as data. Figure 1 shows the principle environment of the localization system. The decentralized setup of our localization system works without a central control unit and is easy to install. The parameters of the system are estimated online in the application.

B. Line Of Sight Condition

Multipath propagation of the signal causes interference of the signal in constructive and destructive manner. As a result, the estimation of TDOA has a higher variance and this decreases the localization accuracy. To overcome the multipath

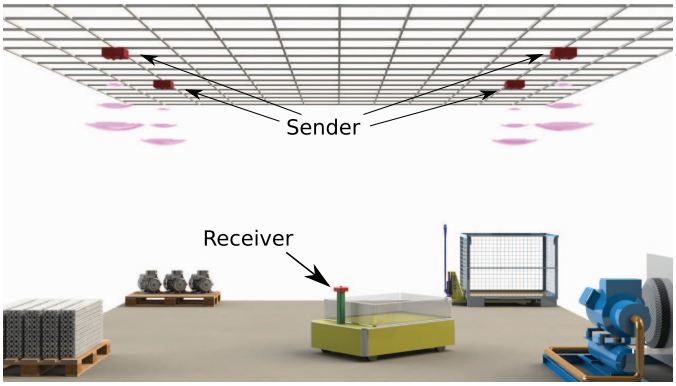

Figure 1. Graph of the localization environment. Reprinted by permission from [3]

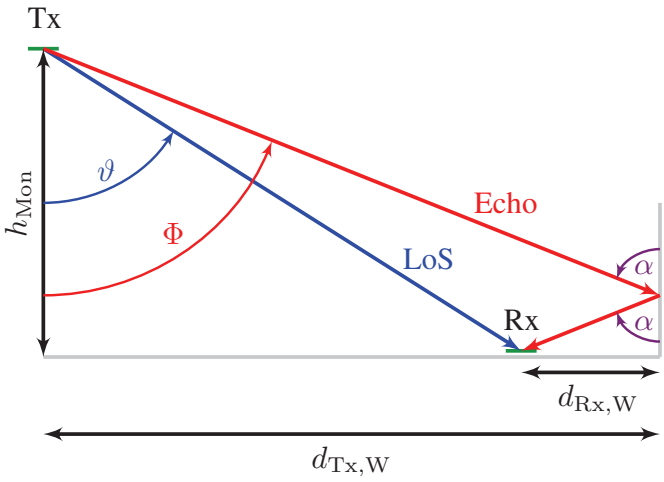

Figure 2. Graph of the line of sight and the multipath propagation.

case, we design our system to work on the line of sight (LOS) signal. Hence, we need a very short signal pulse. In addition, to achieve high data rate and keep the pulse short, we use OFDM to divide the data stream on two carriers. Further, the echo free time τ_{ef} depends on the mounting height of the sender h_{Mon}, the distance $d_{Tx,w}$ of the sender Tx to the next wall w and the distance $d_{Rx,w}$ of the receiver Rx to the next wall w. Figure 2 shows the environment for the echo free calculation. As a result, the echo free time is calculated as:

$$\tau_{ef} = v_s \left(d_{Rx,w} + d_{Tx,w}\right) \sqrt{1 + \frac{h_{\mathrm{Mon}}}{d_{Rx,w} + d_{Tx,w}}} - v_s \sqrt{h_{\mathrm{Mon}}^2 + \left(d_{Tx,w} - d_{Rx,w}\right)^2}\,.$$

To receive interference free signal, the echo free time should be in minimum the size of the transmission packet. The packet size has a transmission duration of 2.1 ms. Therefore, the echo free time should be more than 2 ms. Figure 3 shows the boundary for echo free reception for different mounting heights. Points below the curve indicate interference of the signal by an echo. Indeed, points above the curve guarantee echo free reception.

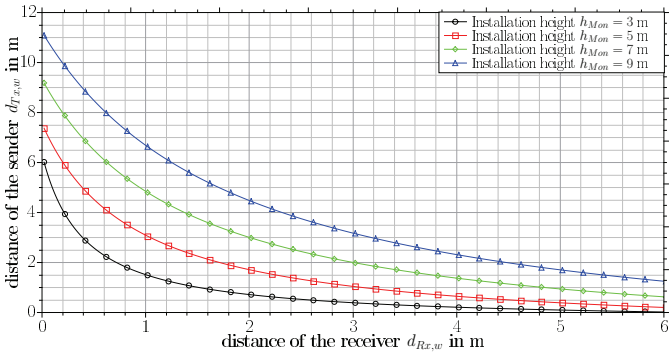

Figure 3. Figure for minimum distance for echo-free reception of 2 ms packet length.

C. Sender

The sender is designed to be powered by photovoltaic. Therefore, the signal is generated by a low power micro-controller. The power consumption is about 10 mW for a transmission of 1 packet per second. Hence, the senders can be powered by a indoor photovoltaic cell with 98 cm^2 (about 10×10 cm^2) [27].

The data is coded and divided into two data streams. Further, the data is mapped by π/4-DQPSK on the both carrier frequencies ($f_0 = 38.8$ kHz and $f_1 = 40.8$ kHz) and the digital-to-analog-converter (DAC) generates the analog signal for the piezo-electric transducers. Figure 4 shows the schematic function and a photo of the sender.

D. Receiver

The receiver includes the analog signal condition and the signal processing with a microcontroller. Therefore, the piezo-electric transducer receives the transmitted ultrasound signal on both carrier frequencies. Further, the power meters triggers the microcontroller to digitize the received signal by an analog-to-digital converter (ADC). Moreover, the signal processing includes the separation of the two data carrier frequencies, the estimation of the synchronization (the time of arrival) and the estimation of the data. Figure 4 shows the schematic function and a photo of the receiver. The receiver is matched to receive both carrier frequencies with same amplitude to ensure equal dynamic range of the ADC for both carrier frequencies [28].

E. Frame Synchronization

We propose two synchronization methods for precise frame synchronization with multiple carriers. Both methods use the phase of both carrier signals. Hence, the phase of the signals is calculated by correlation of the received signal with the reference signal. For carrier $k \in 1, 2$ with frequency f_k the phase at sample position n with a correlation of N samples and sampling frequency f_{sample} is

$$\phi_k(n) = \arg\left[\sum_{x=1}^{N} r_d(x+n) \cdot \mathrm{e}^{j2\pi \cdot f_k \cdot x / f_{\mathrm{sample}}}\right]. \quad (1)$$

Further, the phase difference is calculated between both phases

$$\phi_D(n) = \phi_1(n) - \phi_2(n) \quad (2)$$

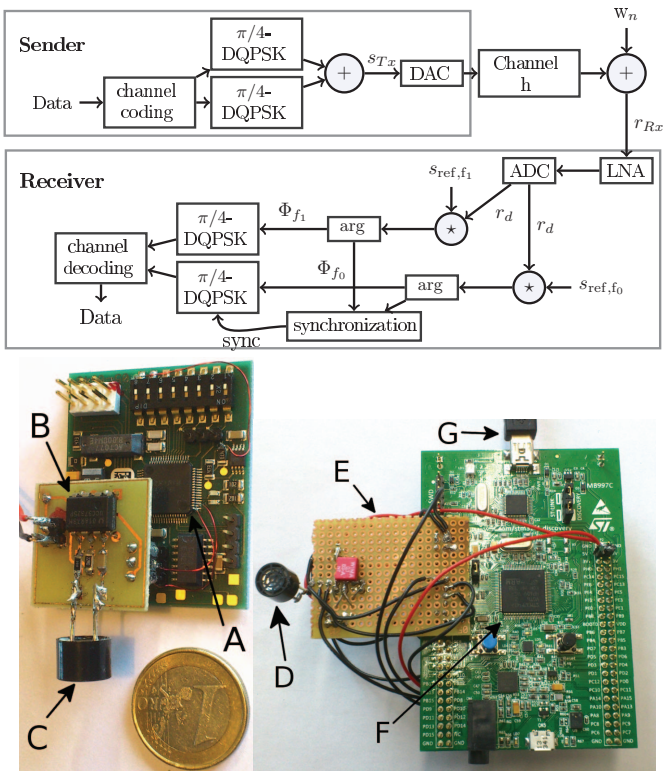

Figure 4. Schematic diagram of the transmission path (top) and photo of the sender (bottom left) and the receiver (bottom right). The micro-controller (A) generates the analog signal, which is amplified (B) and transformed by the piezo-electric transducer (C) to an acoustic signal. On the receiver, the piezo-electric transducer (D) transforms the acoustic signal into electrical signals. Further, the signal is amplified (E) and processed in the ARM STM32F407 micro-controller (F). The decoded identification number is transmitted to the PC (G) for the position calculation.

The first method to estimate the synchronization is to search the point where the function crosses the abscissa:

$$n_{\text{sync}} = \arg\min_{n} \left[|\phi_D(n)| \right] . \tag{3}$$

This is typically done by taking the absolute and search the minimum. Figure 5 demonstrate the principle of the synchronization.

The second method searches the maximum for the correlation of the estimated phase difference with a reference phase $\phi_{Dr}(x)$. Which is equivalent to calculate the variance of the signal in a given time window with M samples:

$$n'_{\text{sync}} = \arg\max_{n'} \sum_{x=1}^{M} \left(\phi_D(x+n') - \bar{\phi}_D(n') \right) \phi_{Dr}(x) \tag{4}$$

with the mean of the measured signal

$$\bar{\phi}_D(n') = \frac{1}{N} \sum_{m=1}^{N} \phi_D(n'+m) . \tag{5}$$

1) Cramér-Rao Lower Bound: We determine the Cramér-Rao Lower Bound (CRLB) for the frame synchronization with multiple frequencies [29] to

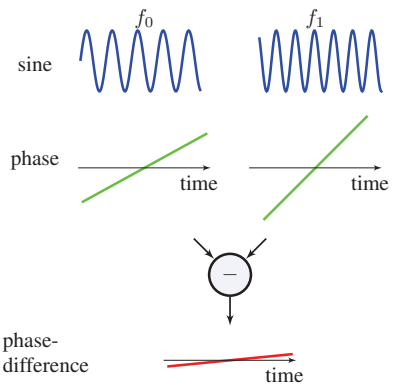

Figure 5. Principle of the phase difference synchronization method

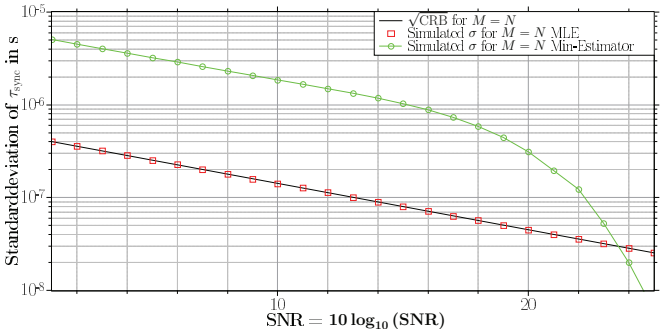

Figure 6. CRLB for phase difference synchronization of two carriers.

$$\text{Var}(d) \geq \frac{v^2}{2\pi^2 \cdot \text{SNR} \cdot f_{\text{sample}}^2} \tag{6}$$

Hence, for a SNR of 10 dB and a sampling frequency of $f_{\text{sample}} = 500\,\text{kHz}$ the minimum standard deviation for the distance estimation is $\sqrt{\text{Var}(d)} \approx 4.7 \cdot 10^{-5}\,\text{m}$. The CRLB is derived for the Maximum Likelihood Estimator (MLE) from Equation (4).

2) Simulation: We evaluate the calculation of the lower bounds for the frame synchronization accuracy. Figure 6 shows the simulation results for a sampling frequency of $f_{\text{sample}} = 500\,\text{kHz}$ and $M = N$. The non linear estimator in Equation (3) outperforms the MLE in Equation (4) for high SNR. Nevertheless, for low SNR the non linear estimator lacks of precision and has a bias error.

F. Distance Measurements

To determine the performance of the ultrasound system we measure the accuracy of the distance measurement between the receiver and one sender. Therefore, we put the sender and receiver pair in a straight line and send in a constant interval the same package. The receiver demodulates the data and measure the TDOA between the packages. Figure 7 shows the TDOA measurement error for a SNR of 10 dB. Although, the measurement error depends on the synchronization of the frame. Hence, for stationary measurements without moving,

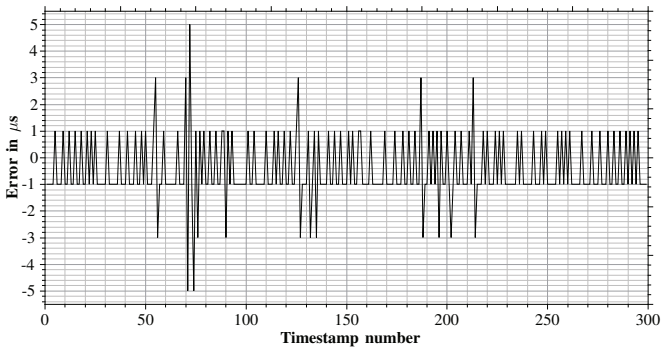

Figure 7. Graph of the synchronization errors at 10 dB SNR.

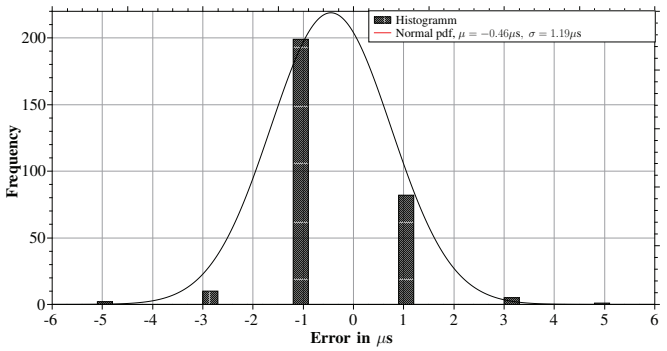

Figure 8. Histogram of the unbiased synchronization errors at 10 dB SNR.

the TDOA errors are the synchronization errors. Figure 8 shows the histogram of the synchronization errors.

As a result, the variance of the synchronization error is about $1.43 \cdot 10^{-12}$ s and the standard deviation about $1.19\,\mu$s. Which results in a distance error of 0.4 mm for a signal velocity of 340 m/s. Though, the standard deviation of a 500 kHz sampled signal is about $5.8 \cdot 10^{-7}$ s respectively 0.2 mm [29] . Thus, the measurement system limits the precision to 0.2 mm.

IV. TDOA Localization

A. Introduction

Once the reception times are precisely estimated by the system described in the previous chapters, the pose of a moving receiver can be tracked using recursive state estimation algorithms, as proved in [26]. However, their performance depends highly upon the knowledge of the initial values of the state. Consequently, it is mandatory to do the localization in two phases: the *calibration phase*, which estimates all the variables of the scenario and the *tracking phase*, which tracks the position of a continuously moving receiver.

The localization scenario consists of B stationary senders which are placed randomly at unknown positions $\mathbf{S}_j$ $(1 \leq j \leq B)$ in a two-dimensional Euclidean space. Every sender emits discrete signals at regular points in time at a fixed interval I_j. The interval may differ from sender to sender. The sending time of the k_j-th signal at sender position $\mathbf{S}_j$ is then described by

$$t_{k_j j} = t_{0j} + k_j I_j \ , \qquad (k_j > 0). \tag{7}$$

The receiver $\mathbf{M}$ moves with a random trajectory in the two-dimensional Euclidean space. Furthermore, we assume that a k_j-th signal of sender $\mathbf{S}_j$ propagates in a straight line from the sender to the receiver and is received at time point

$$T_{k_j j} = \frac{1}{c}\|\mathbf{M} - \mathbf{S}_j\| + t_{k_j j}, \tag{8}$$

where c is the signal velocity and $\|\cdot\|$ denotes the Euclidean norm.

The senders are assumed to be unsynchronized, i.e the intervals I_j and the initial send time t_{0j} varies from sender to sender. Consequently, there is an unknown time offset which relates to the send time between the senders y and j :

$$\delta_{yj} = t_{0,y} - t_{0,j} = (t_{k_y y} - k_y I_y) - (t_{k_j j} - k_j I_j) \tag{9}$$

Since the offsets are transitive, only $B-1$ offsets need to be estimated relative to one sender.

Considering the case where the receiver is continuously moving, signals are received at different positions. This results in the following hyperbolic equation in which two signals, originating from two different senders $\mathbf{S}_y$ and $\mathbf{S}_j$, are received at the positions $\mathbf{M}_{k_y y}$ and $\mathbf{M}_{k_j j}$:

$$\frac{1}{c}(\|\mathbf{M}_{k_y y} - \mathbf{S}_y\| - \|\mathbf{M}_{k_j j} - \mathbf{S}_j\|) = \Delta t_{yj} + \delta_{yj} \ , \tag{10}$$

where Δt_{yj} represents the unsynchronized time difference of arrival of the two signals originated by $\mathbf{S}_y$ and $\mathbf{S}_j$, which may be calculated based on the reception times and the intervals as

$$\Delta t_{ij} = (T_{k_y y} - T_{k_j j}) - (k_y I_y - k_j I_j)\,. \tag{11}$$

B. Tracking phase

During the *tracking phase* the unscented Kalman filter [30] and the particle filter [31] are used. They are both recursive Bayesian estimators [32] based on the Markov assumption. This means the current state $\mathbf{x}_t$ is assumed to depend only on the previous state $\mathbf{x}_{t-1}$. The unscented Kalman filter takes advantage of the knowledge of the noise factors involved in the system to estimate a Gaussian probability distribution of the state. The non-linear functions, like the ones used in TDOA, are linearized in the *unscented transform* [32], [33]. The particle filter uses a set of particles to represent a state hypothesis, approximating the current belief.

In our case the state vector contains the position of the receiver $\mathbf{M}_t$ and the receiver velocity $\mathbf{V}_t$. Besides, in order to estimate the reception time, the offsets relative to one sender $(\delta_{12}, ..., \delta_{1B})$ and its sending time $t_{k_1 1}$ are also estimated. Without loss of generality is defined $\delta_j = \delta_{1j}$ where $\delta_1 = 0$. In conclusion, the state vector is formulated as follows:

$$\mathbf{x}_t = \left(\mathbf{M}_t^T, \mathbf{V}_t^T, t_{k_1 1}, \delta_2, ..., \delta_B\right)^T \ . \tag{12}$$

The measurement is then estimated by the sensor model, which relates the predicted measurement $\overline{z_{k_j}}$ and the state vector:

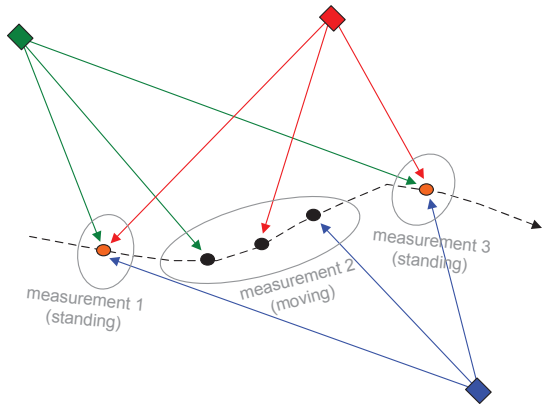

Figure 9. Schematic of the under-determined equation system. If the receiver moves continuously, for every new measurement there are two new variables to estimate only for its position. On the other hand, if the receiver stops receiving one signal from every sender there are B constrains for every two position variables.

$$\overline{z_{k_j}} = \frac{1}{c}\|\mathbf{M}_t - \mathbf{S}_j\| + (t_{k_1 1} + \delta_j) \ . \tag{13}$$

More information about the *tracking phase* can be found in [26].

C. Stop-and-go motion

The continuous movement of the receiver results in a system of equations of the form of Equation (10). The length of the intervals I_y, I_j can be easily computed by receiving two or more successive signals $k_1, k_2, k_1 \neq k_2$, emitted by the same sender while it is temporarily stationary:

$$\begin{aligned} I_y &= \frac{1}{k_1 - k_2}(T_{k_1 y} - T_{k_2 y}) \\ I_j &= \frac{1}{k_1 - k_2}(T_{k_1 j} - T_{k_2 j}) \ . \end{aligned} \tag{14}$$

Then, assuming the intervals I_y and I_j are known, there exist $2P + 2B + (B-1)$ unknown variables after P received signals. Consequently, the equation system is under-determined and cannot be solved in closed form without further information or assumptions on the scenario. Therefore, it is required either to know the initial values of the variables and model their changes (*tracking phase*) or to make special assumptions on the scenario (*calibration phase*). When recursive state estimation algorithms lack of information and are not capable of tracking the pose of a moving receiver, we assume it stops in q different positions $\mathbf{H}_i$, then we have time to receive at least one signal from every sender (*stop-and-go motion*). Doing this, it is only required to estimate one receiver position for every B received signals, which reduces notably the uncertainty and makes possible an uniquely determined system of equations (cf. Fig. 9).

Being $\mathbf{H}_i$ the receiver position when the u-th signal from the first sender T_{u,k_1} is received and $\mathbf{H}_p$ the receiver position when the v-th signal T_{v,k_j} from the other senders is received, we obtain a system of hyperbolic equations of the form:

$$\begin{aligned} f_{u,v} = &\|\mathbf{H}_i - \mathbf{S}_1\| - \|\mathbf{H}_p - \mathbf{S}_j\| \\ &-c(T_{u,k_1} - T_{v,k_j}) + \Delta t_{1j} \end{aligned} \tag{15}$$

where $2 \leq j \leq B$ and $1 \leq p, i \leq q$. The unsynchronized time difference of arrival between two signals, originated by the sender 1 and the sender j, is represented with Δt_{1j}:

$$\Delta t_{1j} = c(k_1 I_1 - k_j I_j + \delta_j) \ . \tag{16}$$

The system of equations has now qB independent equations, which has to be higher than the number of variables:

$$qB \geq \underbrace{2q}_{\text{Receiver}} + \underbrace{2(B-1)}_{\text{Senders}} + \underbrace{B-1}_{\text{Offsets}} \tag{17}$$

Which means the system of equations can be solved in a closed form if the number of standing still positions q is higher than:

$$q \geq \frac{3B-3}{B-2} \tag{18}$$

The stop phase is detected by ensuring that the time difference between two measurements of the same sender is a multiple of the interval plus a certain error due to the measurement noise. To reduce the effect of noise in the measurements, which could lead to wrong detections, an unscented Kalman filter is used. Each component of the estimated state $\mathbf{x}_t$ is the time difference minus the elapsed intervals a of every sender:

$$\mathbf{x}_t = (\rho_{1,t}, \rho_{2,t}, ..., \rho_{B,t})^T \tag{19}$$

where

$$\rho_{j,t} = (T_{k_j j} - T_{(k-a)_j j}) - a I_j \ . \tag{20}$$

If the receiver is standing during a intervals ρ_j is zero plus a certain error. The motion model assumes the receiver does not move. Its movement is undetermined, which is modeled by Gaussian noise with a covariance matrix Σ_Q. The equation which relates the current state with the previous state is then:

$$\rho_{j,t+1} = \rho_{j,t} + \xi \qquad \xi \sim \mathcal{N}(0, \Sigma_Q) \ . \tag{21}$$

The sensor model with relation to the state and the expected measurement $\overline{z_{k_j}}$ is:

$$\overline{z_{k_j}} = \rho_{j,t} + T_{(k-a)_j j} + a I_j + \zeta \qquad \zeta \sim \mathcal{N}(0, \Sigma_N) \tag{22}$$

where Σ_N is the covariance matrix of the measurement noise.

D. Calibration phase

Assuming the *stop-and-go* motion and having a number of standing positions and senders fulfilling Equation (18) the system of hyperbolic equations can be solved with local optimization algorithms. We use both the gradient descent and the Gauss-Newton method, the two are first-order methods that use the derivative of the system of hyperbolic error equations.

Once the timestamps corresponding with the time when the receiver is standing are selected, we can extend the approach in [25] to unsynchronized senders. For simplicity and better understanding we assume that there are G selected signals

from every sender. Then, the Equation (15) results in a quadratic objective which can be formulated as follows:

$$\sum_{u=1}^{G}\sum_{v=1}^{G(B-1)} \underset{\mathbf{H}_{1:q},\mathbf{S}_{2:B},\delta_{2:B}}{\arg\min} (f_{u,v})^2 \ . \tag{23}$$

Which in vector notation is proportional to $w = \frac{1}{2}\mathbf{b}^T\mathbf{b}$ with $\mathbf{b} = (f_{1,1}, ..., f_{G,G(B-1)})^T$. The operator $(\cdot)^T$ denotes the transposition.

We calculate the direction of the steepest ascent:

$$\nabla w = \nabla\left(\frac{1}{2}\mathbf{b}^T\mathbf{b}\right) = \mathbf{Q}^T\mathbf{b} \tag{24}$$

where $\mathbf{Q}$ is the Jacobian matrix:

$$\mathbf{Q} = \begin{bmatrix} \frac{\partial f_{1,1}}{\partial \mathbf{S}_2} & \cdots & \frac{\partial f_{G,G(B-1)}}{\partial \mathbf{S}_2} \\ \vdots & \ddots & \vdots \\ \frac{\partial f_{1,1}}{\partial \mathbf{S}_B} & \cdots & \frac{\partial f_{G,G(B-1)}}{\partial \mathbf{S}_B} \\ \frac{\partial f_{1,1}}{\partial \mathbf{H}_1} & \cdots & \frac{\partial f_{G,G(B-1)}}{\partial \mathbf{H}_1} \\ \vdots & \ddots & \vdots \\ \frac{\partial f_{1,1}}{\partial \mathbf{H}_q} & \cdots & \frac{\partial f_{G,G(B-1)}}{\partial \mathbf{H}_q} \\ \frac{1}{c}\frac{\partial f_{1,1}}{\partial \delta_2} & \cdots & \frac{1}{c}\frac{\partial f_{G,G(B-1)}}{\partial \delta_2} \\ \vdots & \ddots & \vdots \\ \frac{1}{c}\frac{\partial f_{1,1}}{\partial \delta_B} & \cdots & \frac{1}{c}\frac{\partial f_{G,G(B-1)}}{\partial \delta_B} \end{bmatrix}^T \tag{25}$$

The partial derivative with respect to a vector is defined as the derivative with respect to each of its components:

$$\frac{\partial f_{u,v}}{\partial \mathbf{H}_i} = \left(\frac{\partial f_{u,v}}{\partial H_{i,x}}, \frac{\partial f_{u,v}}{\partial H_{i,y}}\right)^T \tag{26}$$

In our case they are calculated as follows:

$$\begin{aligned} \frac{\partial f_{u,v}}{\partial \delta_j} &= c \\ \frac{\partial f_{u,v}}{\partial \mathbf{S}_j} &= \frac{\mathbf{H}_p - \mathbf{S}_j}{\|\mathbf{H}_p - \mathbf{S}_j\|} \end{aligned} \tag{27}$$

When the compared timestamps correspond to the same receiver position ($\mathbf{H}_i = \mathbf{H}_p$) the partial derivative with respect to the receiver position is:

$$\frac{\partial f_{u,v}}{\partial \mathbf{H}_i} = \frac{\partial f_{u,v}}{\partial \mathbf{H}_p} = \frac{\mathbf{H}_i - \mathbf{S}_1}{\|\mathbf{H}_i - \mathbf{S}_1\|} - \frac{\mathbf{H}_p - \mathbf{S}_j}{\|\mathbf{H}_p - \mathbf{S}_j\|} \tag{28}$$

In all other cases the partial derivatives are:

$$\begin{aligned} \frac{\partial f_{u,v}}{\partial \mathbf{H}_i} &= \frac{\mathbf{H}_i - \mathbf{S}_1}{\|\mathbf{H}_i - \mathbf{S}_1\|} \\ \frac{\partial f_{u,v}}{\partial \mathbf{H}_p} &= -\frac{\mathbf{H}_p - \mathbf{S}_j}{\|\mathbf{H}_p - \mathbf{S}_j\|} \end{aligned} \tag{29}$$

All the variables which need to be estimated are components of the state vector $\mathbf{u}$:

$$\mathbf{u} = (\mathbf{S}_2^T, ..., \mathbf{S}_B^T, \mathbf{H}_1^T, ..., \mathbf{H}_q^T, c\delta_2^T, ..., c\delta_B^T)^T \tag{30}$$

Hence, we estimate $c\delta_j$ to have all the variables in the same units (meters) instead of estimating δ_j. Every iteration the state vector is updated using $\mathbf{Q}$ and $\mathbf{b}$. The methods used are:

1) The Gradient Descent Method: In every iteration step l the Gradient Descent method updates the state vector in direction of the steepest descent. The adaptive factor γ sets the step width.

$$\begin{aligned} \hat{\mathbf{u}} &= \gamma\nabla w = \gamma\mathbf{Q}^T\mathbf{b} \\ \mathbf{u}^{l+1} &= \mathbf{u}^l - \hat{\mathbf{u}} \end{aligned} \tag{31}$$

2) The Gauss-Newton Algorithm: Instead of relying on an adaptive factor γ it calculates the step size using the inverse $(\mathbf{Q}^T\mathbf{Q})^{-1}$ for every iteration:

$$\mathbf{u} = (\mathbf{Q}^T\mathbf{Q})^{-1}(\mathbf{Q}^T\mathbf{b}) \tag{32}$$

We calculate for higher numerical stability the pseudo-inverse with singular value decomposition instead of calculating the inverse.

This algorithm is faster, nevertheless it is very prone to divergence when applied to random initial positions. However, it can be used when the Gradient Descent error function has become steady to reduce notably the number of iterations [34].

V. Simulation Results

We implement the local optimization algorithms in Scilab and evaluate them by two different experiments. In both of them the receiver moves in an experiment area of 10 m ×10 m with a velocity of 1.5 m/s. The senders are located at remote positions of a three-dimensional field (Table II), to reduce the effect of adverse sender locations. A Gaussian distributed error with standard deviation of σ_ξ = 0.2 ms is added to the reception times.

The senders have a certain altitude with respect to the receiver. In order to fulfil the two-dimensional assumption, this altitude is assumed to be known and it is not estimated with the local optimization algorithms. Further research will be needed to avoid the Dilution of precision (DOP) when estimating the altitude, as a large change in the height of the senders would lead to only a small change in the TDOA.

Each time a signal is received, it is passed through the unscented Kalman filter. To detect whether the receiver is moving or standing still, the sum of squares of the state vector components is calculated. We assume that the receiver is standing still if the sum of squares is under a threshold ε:

$$\sum_{j=1}^{B} \tau_{j,t}^2 < \varepsilon \tag{33}$$

Figure 10 shows the sum of squares of the signal with and without filtering. Further, it shows the sum of squares of the signal without any noise. Thus, the filtered time difference increases and decreases slower than the others, this is due to the fact that the UKF is acting as a low pass filter. Consequently, if we use the threshold with the filtered signal and the signal is below the threshold, we would suppose that the receiver is standing still when it is already moving. Hence, the last signals are rejected for every standing still position.

In the *first simulation* we assume that the sender positions are estimated beforehand using statistical methods such as the

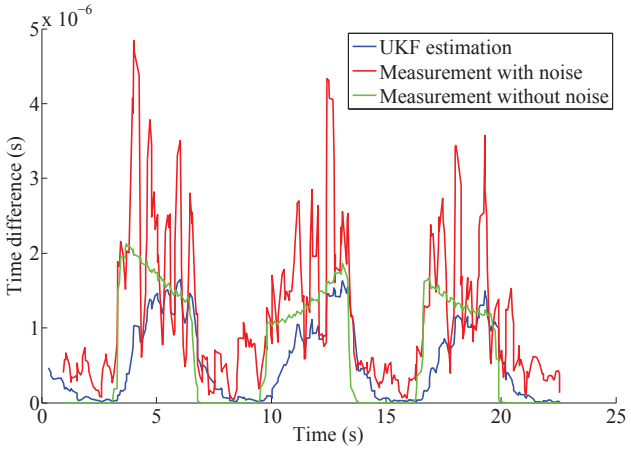

Figure 10. Sum of squares of the time difference with additive noise, the estimated time difference and the time difference without noise. The measured time difference is considerably affected by the noise, which could induce to wrong detections. On the other hand, the UKF estimation is much less affected by the noise although it is delayed.

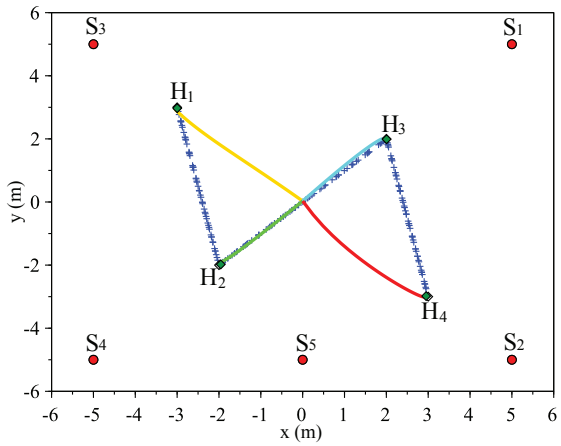

Figure 11. Estimated two-dimensional variables x and y with local optimization. The crosses represent the receiver position when signals arrive.The sender positions (red circles) are assumed to be known. The algorithm estimates the positions where the receiver is standing $\mathbf{H}_1$, $\mathbf{H}_2$, $\mathbf{H}_3$ and $\mathbf{H}_4$. The error between the estimated (solid lines) and the real value reduces in every step.

the Ellipsoid TDOA method [35]. The receiver stops for 3 seconds in 4 different positions. The offsets are initialized assuming the mean of these positions is the center of the field ($\mathbf{H}_c$). Accordingly, the initial offsets are calculated as follows:

$$\forall j : t_{0,j} = \frac{1}{G}\sum_{u=1}^{G}\left(T_{u,k_j} - k_j I_j - \frac{1}{c}\|\mathbf{H}_c - \mathbf{S}_j\|\right) \qquad (34)$$
$$\forall j > 1 : \delta_j = t_{0,1} - t_{0,j}$$

The estimated receiver positions are initialized with random vectors around the center of the experiment area. Figure 11 shows the real standing still positions, the estimated ones in every iteration, and the positions during the movement of the receiver. After the last iteration the mean error is 3.5 cm. Figure 12 shows the estimated offsets in every iteration. The mean error after the last iteration is 0.07 ms.

The algorithm stucks in a local minima when we estimate all the variables without any knowledge. However, if the sender positions are approximately known the algorithm is capable of correcting them and estimating the other variables.

In the *second simulation* the sender positions are assumed to be known with a mean error of 0.60 m. First, assuming these positions are correct, the receiver positions and the offsets are estimated, as it is done in the *first simulation*. Afterwards, the estimated receiver positions and offsets and the known sender positions are used to initialize the algorithm, which corrects them. The result of this correction is shown in Figure 13. In this experiment the receiver stops 6 times in order to increase the number of constrains and have a uniquely determined system of equations.

The mean error of the estimated receiver positions after the last iteration is 5.3 cm and the mean error of the estimated sender positions is 5.6 cm. The offsets mean error is 0.11 ms.

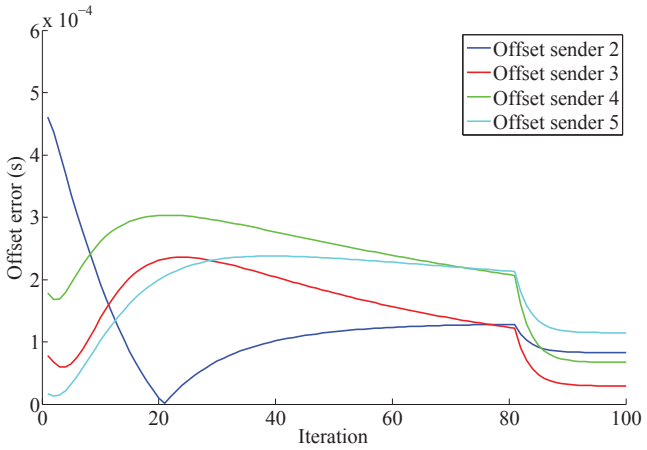

Figure 12. Error between the estimated offsets and the real offsets in every iteration assuming the sender positions are known. The error between the real and the estimated offset is highly reduced after 100 iterations.

VI. Conclusion and Discussion

The synchronization enables high precision indoor localization. We show an accuracy of 0.4 mm for direct distance measurement for 10 dB SNR. Moreover, due to the self-calibration and the photovoltaic powered senders, the installation costs are low. Further, we showed the usage of OFDM to shorten the pulse length and therefore, reduce the interference by echoes. Consequently, we receive the line of sight signal without disturbance and achieve higher precision.

The local optimization algorithms have been proved to be capable of locating with low error the sender positions, their offsets and the standing still receiver locations. The only requirement is to have a rough idea of the sender positions. The period of time when the receiver is not moving is successfully

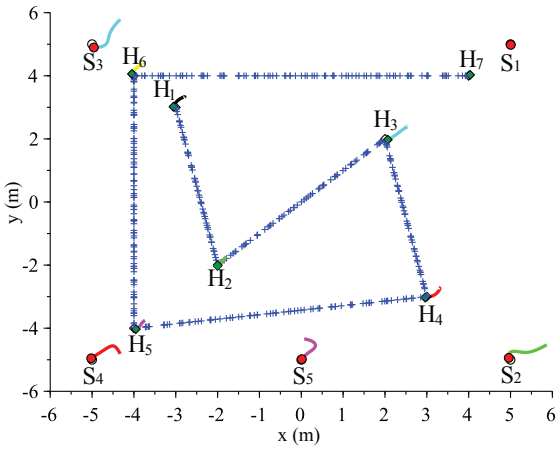

Figure 13. Estimated two-dimensional variables x and y with local optimization. The crosses represent the receiver position when signals arrive. The algorithm corrects the positions where the receiver is standing $\mathbf{H}_1$,$\mathbf{H}_2$,...,$\mathbf{H}_7$ and the sender positions $\mathbf{S}_1$,$\mathbf{S}_2$,...,$\mathbf{S}_5$. The error between the estimated (solid lines) and the real value reduces in every step.

Table II
SENDER POSITIONS AND INTERVAL LENGTHS FOR THE SENDERS USED IN THE LOCAL OPTIMIZATION SIMULATIONS.

	$\mathbf{S}_1$	$\mathbf{S}_2$	$\mathbf{S}_3$	$\mathbf{S}_4$	$\mathbf{S}_5$
Position x (m)	5	5	-5	-5	0
Position y (m)	5	-5	5	-5	-5
Position z (m)	5	5	5	5	5
Interval (s)	0.250	0.275	0.300	0.325	0.350

detected in the presence of Gaussian noise with the aid of an unscented Kalman filter.

Altogether we have all the components for a self-calibration localization system. In the next step we will build a measurement setup with a reference system. Thus we compare the performance of our system with an optical reference system.

ACKNOWLEDGEMENT

This work has been partly supported by the "Spitzencluster MicroTec Suedwest" and German Federal Ministry of Education and Research (BMBF) with the funding number 16SV5988.

REFERENCES

[1] "ISO 9613-1, Acoustics - Attenuation of sound during propagation outdoors - Part1: Calculation of the absorption of sound by the atmosphere," 1993.

[2] T. Stoll, "Dezentral gesteuerter Aufbau von Stetigförderern mittels autonomer Materialflusselemente," Ph.D. dissertation, Karlsruhe Institute of Technology (KIT), 2012.

[3] J. Kokert, F. Hoflinger, and L. Reindl, "Indoor localization system based on galvanometer-laser-scanning for numerous mobile tags (GaLocate)," in *2012 International Conference on Indoor Positioning and Indoor Navigation (IPIN)*, Nov. 2012, pp. 1–7.

[4] F. Höflinger, J. Wendeberg, R. Zhang, M. Bührer, J. Hoppe, A. Bannoura, L. M. Reindl, and C. Schindelhauer, "Acoustic Self-calibrating System for Indoor Smartphone Tracking (ASSIST)," in *Proceedings of 2012 International Conference on Indoor Positioning and Indoor Navigation (IPIN)*, 2012.

[5] A. J. Berni and W. Gregg, "On the utility of chirp modulation for digital signaling," *IEEE Transactions on Communications*, vol. 21, no. 6, pp. 748–751, 1973.

[6] A. Glenn, "Comparison of PSK vs FSK and PSK-AM vs FSK-AM binary-coded transmission systems," *IRE Transactions on Communications Systems*, vol. 8, no. 2, pp. 87–100, Jun. 1960.

[7] K. Murota and K. Hirade, "GMSK modulation for digital mobile radio telephony," *IEEE Transactions on Communications*, vol. 29, no. 7, pp. 1044–1050, 1981.

[8] M. Miller and J. Lee, "BER expressions for differentially detected pi;/4 DQPSK modulation," *IEEE Transactions on Communications*, vol. 46, no. 1, pp. 71–81, 1998.

[9] J. A. C. Bingham, "Multicarrier modulation for data transmission: an idea whose time has come," *IEEE Communications Magazine*, vol. 28, no. 5, pp. 5–14, 1990.

[10] J. M. Villadangos, J. Urena, M. Mazo, A. Hernandez, C. De Marziani, M. Pérez, F. Alvarez, J. García, A. Jimenez, and I. Gude, "Ultrasonic local positioning system with large covered area," in *IEEE International Symposium on Intelligent Signal Processing (WISP)*, October 2007, pp. 935–940.

[11] J. Ureña, A. Hernández, A. Jiménez, J. M. Villadangos, M. Mazo, J. C. García, J. J. García, F. J. Álvarez, C. De Marziani, M. C. Pérez, J. A. Jiménez, A. R. Jiménez, and F. Seco, "Advanced sensorial system for an acoustic LPS," *Microprocessors and Microsystems*, vol. 31, no. 6, pp. 393–401, Sep. 2007. [Online]. Available: http://www.sciencedirect.com/science/article/pii/S0141933107000385

[12] H. Schweinzer and M. Syafrudin, "LOSNUS: an ultrasonic system enabling high accuracy and secure TDoA locating of numerous devices," in *2010 International Conference on Indoor Positioning and Indoor Navigation (IPIN)*, Sep. 2010, pp. 1–8.

[13] D. Ruiz, E. Garcia, J. Urena, D. de Diego, D. Gualda, and J. Garcia, "Extensive ultrasonic local positioning system for navigating with mobile robots," in *10th Workshop on Positioning Navigation and Communication*, 2013.

[14] C. Medina, J. Segura, and A. De la Torre, "A synchronous TDMA ultrasonic TOF measurement system for low-power wireless sensor networks," *IEEE Transactions on Instrumentation and Measurement*, vol. 62, no. 3, pp. 599–611, Mar. 2013.

[15] S. J. Kim and B. K. Kim, "Dynamic ultrasonic hybrid localization system for indoor mobile robots," *IEEE Transactions on Industrial Electronics*, vol. 60, no. 10, pp. 4562–4573, 2013.

[16] M. M. Saad, C. J. Bleakley, T. Ballal, and S. Dobson, "High-accuracy reference-free ultrasonic location estimation," *IEEE Transactions on Instrumentation and Measurement*, vol. 61, no. 6, pp. 1561–1570, Jun. 2012.

[17] G. Shen, R. Zetik, and R. S. Thoma, "Performance Comparison of TOA and TDOA Based Location Estimation Algorithms in LOS Environment," *Proceedings of the 5th workshop on positioning, navigation and communication 2008 (WPNC 08)*, pp. 71–78, 2008.

[18] J. Wendeberg, J. Müller, C. Schindelhauer, and W. Burgard, "Robust Tracking of a Mobile Beacon using Time Differences of Arrival with Simultaneous Calibration of Receiver Positions," in *Proceedings of 2012 International Conference on Indoor Positioning and Indoor Navigation (IPIN)*, 2012.

[19] F. Gustafsson and F. Gunnarsson, "Positioning using time-difference of arrival measurements," in *Acoustics, Speech, and Signal Processing, 2003. Proceedings (ICASSP'03). 2003 IEEE International Conference*, vol. 6, 2003, pp. VI–553.

[20] C. Hongyang, D. Ping, X. Yongjun, and L. Xiaowei, "A Robust Location Algorithm with Biased Extended Kalman Filtering of TDOA Data for Wireless Sensor Networks," in *2005 International Conference on Wireless Communications, Networking and Mobile Computing, 2005. Proceedings.*, vol. 2. IEEE, 2005, pp. 883–886.

[21] R. Zhang, F. Höflinger, and L. Reindl, "TDOA based localization using Interacting Multiple Model estimator and ultrasonic transmitter/receiver," in *Systems, Signals and Devices (SSD), 2012 9th International Multi-Conference on*, march 2012, pp. 1–6.

[22] J. Saloranta and G. Abreu, "Solving the Fast Moving Vehicle Localization Problem via TDOA Algorithms," in *Positioning Navigation and Communication (WPNC), 2011*, 2011, pp. 127–130.

[23] A. Yazici, U. Yayan, and H. Yucel, "An ultrasonic based indoor positioning system," in *Innovations in Intelligent Systems and Applications (INISTA), 2011*. IEEE, 2011, pp. 585–589.

[24] U. Yayan, H. Yucel, and A. Yazıcı, "A low cost ultrasonic based positioning system for the indoor navigation of mobile robots," *Journal of Intelligent & Robotic Systems*, pp. 1–12, May 2014. [Online]. Available: http://link.springer.com/article/10.1007/s10846-014-0060-7

[25] J. Wendeberg, F. Höflinger, C. Schindelhauer, and L. Reindl, "Calibration-Free TDOA Self-Localization," *Journal of Location Based Services*, 2013.

[26] J. Bordoy, P. Hornecker, J. Wendeberg, R. Zhang, C. Schindelhauer, and L. Reindl, "Robust tracking of a mobile receiver using unsynchronized time differences of arrival," in *2013 International Conference on Indoor Positioning and Indoor Navigation (IPIN)*, 2013.

[27] R. Karola and Kasemann, "Selection and dimensioning of photovoltaic harvester for wireless sensor systems," in *ITG/GMA Symposium; Proceedings of Sensors and Measuring Systems 2014; 17*, Nürnberg, Germany, Jun. 2014.

[28] A. Ens and L. M. Reindl, "Wide-band piezo-electric ultrasound transceiver matching," in *ITG/GMA Symposium; Proceedings of Sensors and Measuring Systems 2014; 17*, Jun. 2014, pp. 1–4.

[29] A. Ens, L. M. Reindl, C. Schindelhauer, and T. Janson, "Robust multicarrier frame synchronization for localization systems with ultrasound," in *Proc. of the 18th International OFDM Workschop (InOWo'14) 2014*, Essen, Gremany, Aug. 2014.

[30] S. J. Julier and J. K. Uhlmann, "New Extension of the Kalman Filter to Nonlinear Systems," in *AeroSense'97*. International Society for Optics and Photonics, 1997, pp. 182–193.

[31] S. Thrun, D. Fox, W. Burgard, and F. Dellaert, "Robust Monte Carlo Localization for Mobile Robots," *Artificial Intelligence*, vol. 128, no. 1-2, pp. 99–141, 2000.

[32] S. Thrun, W. Burgard, and D. Fox, *Probabilistic Robotics*. mitpress, 2005.

[33] S. J. Julier and J. K. Uhlmann, "Unscented Filtering and Nonlinear Estimation," *Proceedings of the IEEE*, vol. 92, no. 3, pp. 401–422, 2004.

[34] J. Wendeberg, "Calibration-free localization using time differences of arrival," Ph.D. dissertation, Albert-Ludwigs-Universität Freiburg, 2013.

[35] J. Wendeberg, T. Janson, and C. Schindelhauer, "Self-Localization based on Ambient Signals," *Theoretical Computer Science*, vol. 453, pp. 98–109, 2012.